Progress In Electromagnetics Research M, Vol. 47, 181–189, 2016

Study of UPML Absorbing Boundary Condition for the Five-Step LOD-FDTD Method

Lixia Yang[1, *], Xuejian Feng[1], and Lunjin Chen[2]

Abstract—In this paper, the uniaxial anisotropic perfectly matched layer (UPML) absorbing boundary condition in unconditionally stable five-step locally one-dimensional finite-difference time-domain (LOD5-FDTD) method is deduced. The UPML absorbing boundary condition (ABC) is validated based on comparison with a simulation in larger domain (and thus without reflection) in the first test. Then using a sinusoidal source, target field phase distribution surrounded by the UPML-ABC is analyzed. The results further illustrate the stability and efficiency of the UPML absorbing boundary condition.

1. INTRODUCTION

The three-dimensional five-step LOD-FDTD (LOD5-FDTD) method [1] is an unconditionally stable method whose time step is not restricted by the Courant-Friedrich-Lewy (CFL) stability condition [2]. It is worth mentioning that the LOD5-FDTD method has second-order accuracy in time domain and yields less numerical dispersion than the ADI-FDTD [3, 4], two-step LOD-FDTD [5], and three-step LOD-FDTD [6] methods.

For application to the simulation of the electromagnetic scattering and propagation in the free-space, the LOD-FDTD method should have an efficient absorbing layer in the computation field. In [7, 8], the split-field perfectly matched layer (PML) and convolution PML have been applied to LOD-FDTD method. And the Mur's and uniaxial anisotropic PML (UPML) absorbing boundary condition [9–12] have been implemented within the two-dimensional LOD-FDTD method [13]. More recently, there are some other PML-ABC applied in the LOD-FDTD method such as LOD-CPML [14] and LOD-SC-PML [15]. In this paper, the UPML-ABC is applied to the LOD5-FDTD method. Using the proposed UPML-ABC, the reflection error of an electric dipole source and target field phase distribution of a sinusoidal source are computed. The results of these simulation experiments show that the UPML-ABC can be used efficiently in the LOD5-FDTD method.

2. FORMULATION

In the UPML medium, the Maxwell's curl equations in frequency domain can be written as follows [9]

$$\nabla \times \vec{H} = j\omega\varepsilon_0\varepsilon_r\bar{\bar{\varepsilon}}\vec{E} \tag{1}$$

$$\nabla \times \vec{E} = -j\omega\mu_0\mu_r\bar{\bar{\mu}}\vec{H} \tag{2}$$

where ε_r and μ_r are the relative permittivity and permeability of the isotropic space, and $\bar{\bar{\varepsilon}}$, $\bar{\bar{\mu}}$ are relative permittivity and permeability tensors, respectively, which can be written as

$$\bar{\bar{\varepsilon}} = \bar{\bar{\mu}} = \begin{bmatrix} \frac{s_y s_z}{s_x} & 0 & 0 \\ 0 & \frac{s_x s_z}{s_y} & 0 \\ 0 & 0 & \frac{s_x s_y}{s_z} \end{bmatrix}, \quad s_Q = \kappa_Q + \frac{\sigma_Q}{j\omega\varepsilon_0}, \quad Q = x, y, z \tag{3}$$

Received 23 February 2016, Accepted 24 March 2016, Scheduled 13 April 2016

* Corresponding author: Lixia Yang (lixiayang@yeah.net).
[1] Department of Communication Engineering, Jiangsu University, Zhenjiang, China. [2] Department of Physics, University of Texas at Dallas, Richardson, USA.

where κ_Q and σ_Q are the attenuation factor and conductivity, respectively.

For the traditional LOD5-FDTD method, first sub-step equations are written as follow [1]

$$E_y^{n+1/6} = E_y^n - \frac{\Delta t}{4\varepsilon}\left(\frac{\partial H_z^n}{\partial x} + \frac{\partial H_z^{n+1/6}}{\partial x}\right) \tag{4}$$

$$E_z^{n+1/6} = E_z^n + \frac{\Delta t}{4\varepsilon}\left(\frac{\partial H_y^n}{\partial x} + \frac{\partial H_y^{n+1/6}}{\partial x}\right) \tag{5}$$

$$H_y^{n+1/6} = H_y^n + \frac{\Delta t}{4\mu}\left(\frac{\partial E_z^n}{\partial x} + \frac{\partial E_z^{n+1/6}}{\partial x}\right) \tag{6}$$

$$H_z^{n+1/6} = H_z^n - \frac{\Delta t}{4\mu}\left(\frac{\partial E_y^n}{\partial x} + \frac{\partial E_y^{n+1/6}}{\partial x}\right) \tag{7}$$

Equations (4)–(7) can be transformed as follows

$$-\frac{2\varepsilon_1}{3}\frac{\partial E_y}{\partial t} = \frac{\partial H_z^n}{\partial x} + \frac{\partial H_z^{n+1/6}}{\partial x} \tag{8}$$

$$\frac{2\varepsilon_1}{3}\frac{\partial E_z}{\partial t} = \frac{\partial H_y^n}{\partial x} + \frac{\partial H_y^{n+1/6}}{\partial x} \tag{9}$$

$$\frac{2\mu_1}{3}\frac{\partial H_y}{\partial t} = \frac{\partial E_z^n}{\partial x} + \frac{\partial E_z^{n+1/6}}{\partial x} \tag{10}$$

$$-\frac{2\mu_1}{3}\frac{\partial H_z}{\partial t} = \frac{\partial E_y^n}{\partial x} + \frac{\partial E_y^{n+1/6}}{\partial x} \tag{11}$$

Then Equations (8)–(11) transform into frequency domain are written as follows

$$-\frac{2}{3}j\omega\varepsilon_1\frac{\partial E_y}{\partial t} = \frac{\partial H_z^n}{\partial x} + \frac{\partial H_z^{n+1/6}}{\partial x} \tag{12}$$

$$\frac{2}{3}j\omega\varepsilon_1\frac{\partial E_z}{\partial t} = \frac{\partial H_y^n}{\partial x} + \frac{\partial H_y^{n+1/6}}{\partial x} \tag{13}$$

$$\frac{2}{3}j\omega\mu_1\frac{\partial H_y}{\partial t} = \frac{\partial E_z^n}{\partial x} + \frac{\partial E_z^{n+1/6}}{\partial x} \tag{14}$$

$$-\frac{2}{3}j\omega\mu_1\frac{\partial H_z}{\partial t} = \frac{\partial E_y^n}{\partial x} + \frac{\partial E_y^{n+1/6}}{\partial x} \tag{15}$$

Then for the UPML medium, the LOD5-FDTD method equations in frequency domain can be written as follows

First sub-step

$$-\frac{2}{3}j\omega\varepsilon_1\frac{s_x s_z}{s_y}E_y = \frac{\partial H_z^n}{\partial x} + \frac{\partial H_z^{n+1/6}}{\partial x} \tag{16}$$

$$\frac{2}{3}j\omega\varepsilon_1\frac{s_x s_y}{s_z}E_z = \frac{\partial H_y^n}{\partial x} + \frac{\partial H_y^{n+1/6}}{\partial x} \tag{17}$$

$$\frac{2}{3}j\omega\mu_1\frac{s_x s_z}{s_y}H_y = \frac{\partial E_z^n}{\partial x} + \frac{\partial E_z^{n+1/6}}{\partial x} \tag{18}$$

$$-\frac{2}{3}j\omega\mu_1\frac{s_x s_y}{s_z}H_z = \frac{\partial E_y^n}{\partial x} + \frac{\partial E_y^{n+1/6}}{\partial x} \tag{19}$$

Second sub-step

$$\frac{2}{3}j\omega\varepsilon_1\frac{s_y s_z}{s_x}E_x = \frac{\partial H_z^{n+1/6}}{\partial y} + \frac{\partial H_z^{n+2/6}}{\partial y} \tag{20}$$

$$-\frac{2}{3}j\omega\varepsilon_1\frac{s_x s_y}{s_z}E_z = \frac{\partial H_x^{n+1/6}}{\partial y} + \frac{\partial H_x^{n+2/6}}{\partial y} \tag{21}$$

$$-\frac{2}{3}j\omega\mu_1\frac{s_y s_z}{s_x}H_x = \frac{\partial E_z^{n+1/6}}{\partial y} + \frac{\partial E_z^{n+2/6}}{\partial y} \tag{22}$$

$$\frac{2}{3}j\omega\mu_1\frac{s_x s_y}{s_z}H_z = \frac{\partial E_x^{n+1/6}}{\partial y} + \frac{\partial E_x^{n+2/6}}{\partial y} \tag{23}$$

Third sub-step

$$-\frac{2}{3}j\omega\varepsilon_1\frac{s_y s_z}{s_x}E_x = \frac{\partial H_y^{n+2/6}}{\partial z} + \frac{\partial H_y^{n+4/6}}{\partial z} \tag{24}$$

$$\frac{2}{3}j\omega\varepsilon_1\frac{s_x s_z}{s_y}E_y = \frac{\partial H_x^{n+2/6}}{\partial z} + \frac{\partial H_x^{n+4/6}}{\partial z} \tag{25}$$

$$\frac{2}{3}j\omega\mu_1\frac{s_y s_z}{s_x}H_x = \frac{\partial E_y^{n+2/6}}{\partial z} + \frac{\partial E_y^{n+4/6}}{\partial z} \tag{26}$$

$$-\frac{2}{3}j\omega\mu_1\frac{s_x s_z}{s_y}H_y = \frac{\partial E_x^{n+2/6}}{\partial z} + \frac{\partial E_x^{n+4/6}}{\partial z} \tag{27}$$

Fourth sub-step

$$\frac{2}{3}j\omega\varepsilon_1\frac{s_y s_z}{s_x}E_x = \frac{\partial H_z^{n+4/6}}{\partial y} + \frac{\partial H_z^{n+5/6}}{\partial y} \tag{28}$$

$$-\frac{2}{3}j\omega\varepsilon_1\frac{s_x s_y}{s_z}E_z = \frac{\partial H_x^{n+4/6}}{\partial y} + \frac{\partial H_x^{n+5/6}}{\partial y} \tag{29}$$

$$-\frac{2}{3}j\omega\mu_1\frac{s_y s_z}{s_x}H_x = \frac{\partial E_z^{n+4/6}}{\partial y} + \frac{\partial E_z^{n+5/6}}{\partial y} \tag{30}$$

$$\frac{2}{3}j\omega\mu_1\frac{s_x s_y}{s_z}H_z = \frac{\partial E_x^{n+4/6}}{\partial y} + \frac{\partial E_x^{n+5/6}}{\partial y} \tag{31}$$

Fifth sub-step

$$-\frac{2}{3}j\omega\varepsilon_1\frac{s_x s_z}{s_y}E_y = \frac{\partial H_z^{n+5/6}}{\partial x} + \frac{\partial H_z^{n+1}}{\partial x} \tag{32}$$

$$\frac{2}{3}j\omega\varepsilon_1\frac{s_x s_y}{s_z}E_z = \frac{\partial H_y^{n+5/6}}{\partial x} + \frac{\partial H_y^{n+1}}{\partial x} \tag{33}$$

$$\frac{2}{3}j\omega\mu_1\frac{s_x s_z}{s_y}H_y = \frac{\partial E_z^{n+5/6}}{\partial x} + \frac{\partial E_z^{n+1}}{\partial x} \tag{34}$$

$$-\frac{2}{3}j\omega\mu_1\frac{s_x s_y}{s_z}H_z = \frac{\partial E_y^{n+5/6}}{\partial x} + \frac{\partial E_y^{n+1}}{\partial x} \tag{35}$$

where $\varepsilon_1 = \varepsilon_0\varepsilon_r$, $\mu_1 = \mu_0\mu_r$. The following six auxiliary variables are defined:

$$D_x = \frac{2}{3}\varepsilon_1\frac{s_z}{s_x}E_x, \quad D_y = \frac{2}{3}\varepsilon_1\frac{s_x}{s_y}E_y, \quad D_z = \frac{2}{3}\varepsilon_1\frac{s_y}{s_z}E_z \tag{36}$$

$$B_x = \frac{2}{3}\mu_1\frac{s_z}{s_x}H_x, \quad B_y = \frac{2}{3}\mu_1\frac{s_x}{s_y}H_y, \quad B_z = \frac{2}{3}\mu_1\frac{s_y}{s_z}H_z \tag{37}$$

Take the first sub-step as an example by substituting Eqs. (36), (37) into Eqs. (16)–(19) and converting the expression from frequency domain to time domain with the aid of $j\omega \to \partial/\partial t$, we obtain the expression for the first sub-step of the five sub-steps:

$$\begin{aligned}
\frac{\partial E_z^n}{\partial x} + \frac{\partial E_z^{n+1/6}}{\partial x} &= \frac{2}{3}\frac{\partial}{\partial t}(s_z B_y) && (38)\\
\frac{\partial E_y^n}{\partial x} + \frac{\partial E_y^{n+1/6}}{\partial x} &= \frac{2}{3}\frac{\partial}{\partial t}(-s_x B_z) && (39)\\
\frac{\partial H_z^n}{\partial x} + \frac{\partial H_z^{n+1/6}}{\partial x} &= \frac{2}{3}\frac{\partial}{\partial t}(-s_z D_y) && (40)\\
\frac{\partial H_y^n}{\partial x} + \frac{\partial H_y^{n+1/6}}{\partial x} &= \frac{2}{3}\frac{\partial}{\partial t}(s_x D_z) && (41)
\end{aligned}$$

Due to implicit nature of the LOD5-FDTD UPML in Eqs. (38)–(41), in their current form, it is computationally expensive to simulate. Therefore, for efficient simulation, these equations are further simplified. By using central difference scheme for time and spatial derivative, we can solve the electric and magnetic field components of the UPML. Here, electric field component $E_y^{n+1/6}$ is shown as follows after putting Eq. (40) into Eq. (39):

$$aE_{y(i-1,j+1/2,k)}^{n+1/6} + bE_{y(i,j+1/2,k)}^{n+1/6} + cE_{y(i+1,j+1/2,k)}^{n+1/6} = d \tag{42}$$

where:

$$\begin{aligned}
a &= -\frac{9}{4}\frac{1}{\mu_1\varepsilon_1(\Delta x)^2}\frac{1}{AAX(i,j+1/2,k)}\frac{1}{AAX(i-1/2,j+1/2,k)}\\
b &= 1+\frac{9}{4}\frac{1}{\mu_1\varepsilon_1(\Delta x)^2}\left(\frac{1}{AAX(i,j+1/2,k)}\frac{1}{AAX(i+1/2,j+1/2,k)}\right.\\
&\qquad \left.+\frac{1}{AAX(i,j+1/2,k)}\frac{1}{AAX(i-1/2,j+1/2,k)}\right)\\
c &= -\frac{9}{4}\frac{1}{\mu_1\varepsilon_1(\Delta x)^2}\frac{1}{AAX(i,j+1/2,k)}\frac{1}{AAX(i+1/2,j+1/2,k)}\\
AAX &= \frac{6\kappa_x}{\Delta t}+\frac{\sigma_x}{2\varepsilon_0}, \quad AAY=\frac{6\kappa_y}{\Delta t}+\frac{\sigma_y}{2\varepsilon_0}\\
AAZ &= \frac{6\kappa_z}{\Delta t}+\frac{\sigma_z}{2\varepsilon_0}, \quad BBX=\frac{6\kappa_x}{\Delta t}-\frac{\sigma_x}{2\varepsilon_0}\\
BBY &= \frac{6\kappa_y}{\Delta t}-\frac{\sigma_y}{2\varepsilon_0}, \quad BBZ=\frac{6\kappa_z}{\Delta t}-\frac{\sigma_z}{2\varepsilon_0}
\end{aligned}$$

Since electric component $E_y^{n+1/6}$ is already known, auxiliary variable $B_z^{n+1/6}$ can be updated with Eq. (38). Then, magnetic component $H_z^{n+1/6}$ can be updated with the third formula of Eq. (37).

$$\begin{aligned}
H_{z(i+1/2,j+1/2,k)}^{n+1/6} &= eH_{z(i+1/2,j+1/2,k)}^{n} + fB_{z(i+1/2,j+1/2,k)}^{n}\\
&\quad +g\left(E_{y(i+1,j+1/2,k)}^{n+1/6} - E_{y(i,j+1/2,k)}^{n+1/6} + E_{y(i+1,j+1/2,k)}^{n} - E_{y(i,j+1/2,k)}^{n}\right)
\end{aligned} \tag{43}$$

where:

$$\begin{aligned}
e &= \frac{BBY(i+1/2,j+1/2,k)}{AAY(i+1/2,j+1/2,k)}\\
f &= \frac{AAZ(i+1/2,j+1/2,k)}{\mu_1 AAY(i+1/2,j+1/2,k)}\frac{BBX(i+1/2,j+1/2,k)}{AAX(i+1/2,j+1/2,k)} - \frac{BBZ(i+1/2,j+1/2,k)}{\mu_1 AAY(i+1/2,j+1/2,k)}\\
g &= -\frac{3}{2}\frac{1}{\Delta x\cdot AAX(i+1/2,j+1/2,k)}\frac{AAZ(i+1/2,j+1/2,k)}{\mu_1 AAY(i+1/2,j+1/2,k)}
\end{aligned}$$

Similar to Eqs. (38)–(43), for the other four sub-steps, the updating electric and magnetic field components can also be derived.

$$
\begin{aligned}
d = &\left\{ \frac{BBX(i,j+1/2,k)}{AAX(i,j+1/2,k)} - \frac{9}{4}\frac{1}{\mu_1\varepsilon_1(\Delta x)^2} \cdot \left(\begin{array}{c} \frac{1}{AAX(i,j+1/2,k)AAX(i+1/2,j+1/2,k)} \\ +\frac{1}{AAX(i,j+1/2,k)AAX(i-1/2,j+1/2,k)} \end{array} \right) \right\} E^n_{y(i,j+1/2,k)} \\
&-\frac{1}{\varepsilon_1}\left(\frac{BBY(i,j+1/2,k)}{AAX(i,j+1/2,k)} - \frac{AAY(i,j+1/2,k)\,BBZ(i,j+1/2,k)}{AAX(i,j+1/2,k)\,AAZ(i,j+1/2,k)} \right) D^n_{y(i,j+1/2,k)} \\
&-\frac{3}{2}\frac{1}{\varepsilon_1\Delta x}\frac{AAY(i,j+1/2,k)}{AAX(i,j+1/2,k)\,AAZ(i,j+1/2,k)} \cdot \left\{ \left(1 + \frac{BBY(i+1/2,j+1/2,k)}{AAY(i+1/2,j+1/2,k)} \right) \right. \\
&\left. H^n_{z(i+1/2,j+1/2,k)} - \left(1 + \frac{BBY(i-1/2,j+1/2,k)}{AAY(i-1/2,j+1/2,k)} \right) H^n_{z(i-1/2,j+1/2,k)} \right\} \\
&+\frac{9}{4}\frac{1}{\mu_1\varepsilon_1(\Delta x)^2}\frac{1}{AAX(i,j+1/2,k)} \cdot \left(\frac{1}{AAX(i+1/2,j+1/2,k)} E^n_{y(i+1,j+1/2,k)} \right. \\
&\left. +\frac{1}{AAX(i-1/2,j+1/2,k)} E^n_{y(i-1,j+1/2,k)} \right) - \frac{3}{2}\frac{1}{\mu_1\varepsilon_1\Delta x}\frac{AAY(i,j+1/2,k)}{AAX(i,j+1/2,k)\,AAZ(i,j+1/2,k)} \\
&\cdot \left\{ \left(\frac{AAZ(i+1/2,j+1/2,k)\,BBX(i+1/2,j+1/2,k)}{AAY(i+1/2,j+1/2,k)\,AAX(i+1/2,j+1/2,k)} - \frac{BBZ(i+1/2,j+1/2,k)}{AAY(i+1/2,j+1/2,k)} \right) B^n_{z(i+1/2,j+1/2,k)} \right. \\
&\left. -\left(\frac{AAZ(i-1/2,j+1/2,k)BBX(i-1/2,j+1/2,k)}{AAY(i-1/2,j+1/2,k)AAX(i-1/2,j+1/2,k)} - \frac{BBZ(i-1/2,j+1/2,k)}{AAY(i-1/2,j+1/2,k)} \right) B^n_{z(i-1/2,j+1/2,k)} \right\}
\end{aligned}
$$

3. NUMERICAL RESULTS

In this section, we use two numerical simulation tests to validate the proposed methods.

In the first test, a point electric dipole source is located at the center of the computation region. A Gaussian pulse $P(t) = 10^{-10}\exp[-((t-3T)/T)^2]$, with $T = 2\,\mathrm{ns}$, is used as the excitation source. The structure of the computation region has $40 \times 40 \times 40$ cells, with 40 cells along each of x, y, and z directions, and the UPML has 10 cells along x, y and z directions. The spatial step is set as $\Delta x = \Delta y = \Delta z = 5\,\mathrm{cm}$.

For the purpose of comparison, a reference solution without UPML-ABC is computed by using a larger domain ($160 \times 160 \times 160$ cells). The relative reflection error is defined as:

$$\delta = 20\log_{10}\left(\frac{|E_z - E_{ref}|}{\max|E_{ref}|} \right) \tag{44}$$

where E_{ref} is electric field at the same observation point for a lager domain without reflection.

CFL number (S) is defined as the ratio of the time step size (Δt) to the CFL limit ($\Delta t_{CFL} = \Delta x/\sqrt{3}/c$):

$$CFLN = \frac{\Delta t}{\Delta t_{CFL}} \tag{45}$$

And the UPML-ABC parameters for implicit LOD5-FDTD method are given as:

$$\sigma_{\max} = 0.9\sigma_{opt}, \quad \kappa_{\max} = 10 \tag{46}$$

where σ_{opt} were given in [9], $\sigma_{opt} = (m+1)/(150\pi\Delta_x\sqrt{\varepsilon_r})$, and m is the order of polynomial scaling. Take x direction as an example,

$$\sigma_x(x) = (x/d)^m \sigma_{x,\max} \tag{47}$$

$$\kappa_x(x) = 1 + (\kappa_{x,\max} - 1) \cdot (x/d)^m \tag{48}$$

where d is the depth of the UPML. The value of σ_x starts with 0 at $x = 0$ (the surface of the UPML) and increases to $\sigma_{x,\max}$ at $x = d$ (the PEC outer boundary) in the UPML. Similarly, for the UPML, κ_x increases ranging from 1 at $x = 0$ to $\kappa_{x,\max}$ at $x = d$ in the UPML [16].

Figure 1 shows the relative error of the three methods observed at CFLN $= 1$. Fig. 1 demonstrates that both LOD5UPML and conventional FDTDUPML have almost the same relative error and nearly -15 dB smaller than the LOD5CPML method on average. For further analysis of the method, Figs. 2–5 show relative error with respect to time for different CFLNs at different observation points. Fig. 2 shows the relative errors with different values of CFLN ($= 1, 4$, and 9) at the observation point $E_z(0, 10\Delta y, 0)$ for LOD5CPML. Fig. 3 shows the relative errors with different values of CFLN ($= 1, 4$, and 9) at the observation point $E_z(0, 10\Delta y, 0)$ for LOD5UPML. Fig. 4 shows the relative errors with different values of CFLN ($= 1, 4$, and 9) at the observation point $E_z(10\Delta x, 10\Delta y, 0)$ for LOD5UPML. And Fig. 5 shows the relative errors with different values of CFLN ($= 1, 4$, and 9) at the observation point $E_z(0, 10\Delta y, 0)$ for LOD5CPML. Fig. 3 shows the relative errors with different values of CFLN ($= 1, 4$, and 9) at the observation point $E_z(0, 10\Delta y, 0)$ for LOD5UPML. Fig. 4 shows the relative errors with different values of CFLN ($= 1, 4$, and 9) at the observation point $E_z(10\Delta x, 10\Delta y, 0)$ for LOD5UPML.

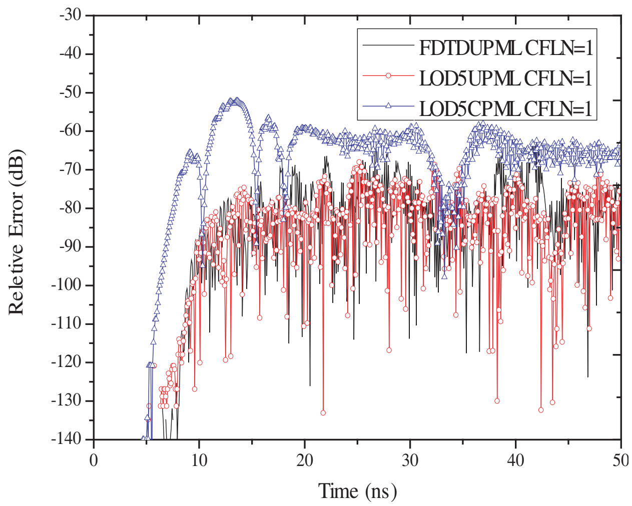

Figure 1. Relative error of the LOD5-FDTD UPML, CPML and conventional FDTD UPML for CFLN $= 1$ at point $E_z(0, 10\Delta y, 0)$.

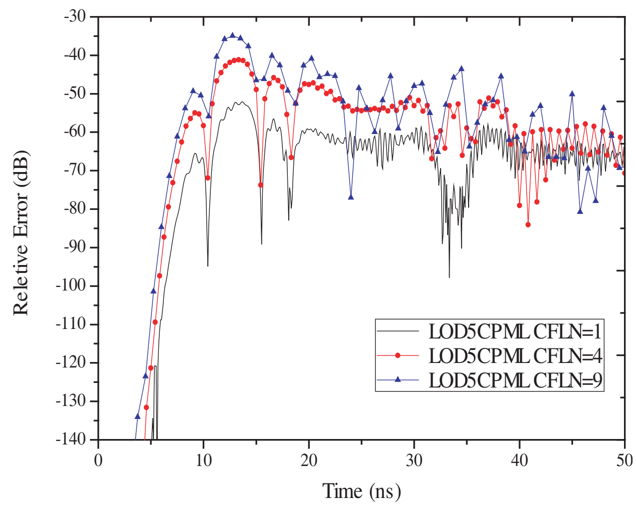

Figure 2. The relative error against time at the observation point $E_z(0, 10\Delta y, 0)$ for LOD5CPML.

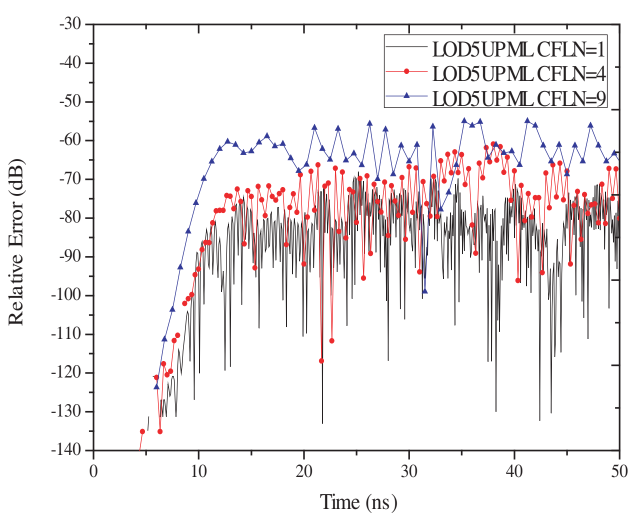

Figure 3. The relative error against time at the observation point $E_z(0, 10\Delta y, 0)$ for LOD5UPML.

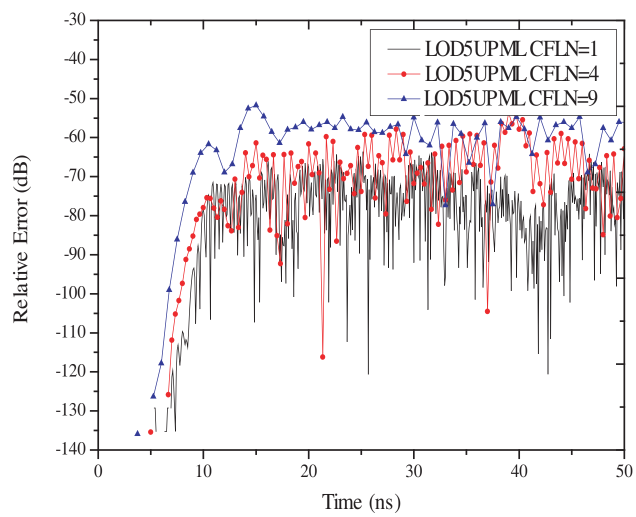

Figure 4. The relative error against time at the observation point $E_z(10\Delta x, 10\Delta y, 0)$ for LOD5UPML.

And Fig. 5 shows the relative errors with different values of CFLN ($= 1, 4$, and 9) at the observation point $E_z(10\Delta x, 10\Delta y, 10\Delta z)$ for LOD5UPML. From Fig. 2 it can be observed that the reflection error is below -35 dB for any CFLN bellow 9 for LOD5CPML. From Fig. 3 and Fig. 4, it can be observed that the reflection error is well below -50 dB for any CFLN bellow 9 for LOD5UPML. And it can be observed from Fig. 5 for any S bellow 9 that the reflection error is well below the maximum value -48 dB for LOD5UPML. Comparing Fig. 2 with Fig. 3, it can also be observed that the relative error of the LOD5UPML is nearly -15 dB smaller than the LOD5CPML on average when CFLN $= 1, 4, 9$ at the observation point $E_z(0, 10\Delta y, 0)$. The refection error performance of all the three observation points illustrates that the proposed UPML-ABC has good absorption effect.

For the second test, target field phase distribution of a sinusoidal source is analyzed with UPML-ABC. The computation region has $160 \times 160 \times 160$ cells. And the computation region is surrounded by additional 10-cell UPML absorbing layers. Excitation source expression is as follows:

$$\mathbf{P}(t) = \hat{e}_z \sin(\omega t), \quad \omega = 2\pi f \tag{49}$$

where $f = 3$ GHz and LOD5-FDTD cell size is $\Delta x = \Delta y = \Delta z = 5$ cm. Fig. 6 shows the radiation

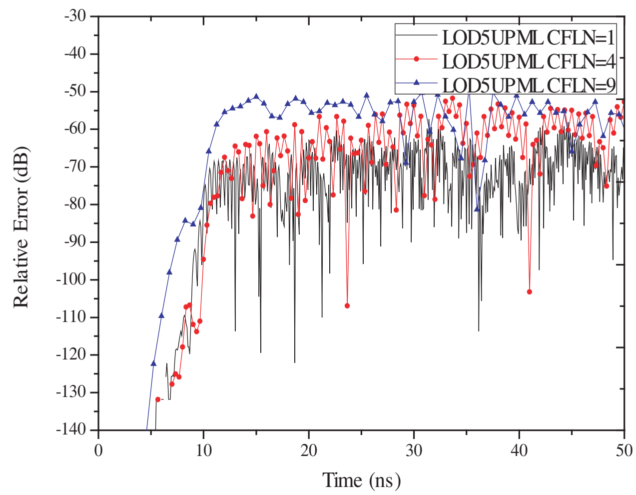

Figure 5. The relative error against time at the observation point $E_z(10\Delta x, 10\Delta y, 10\Delta z)$ for LOD5UPML.

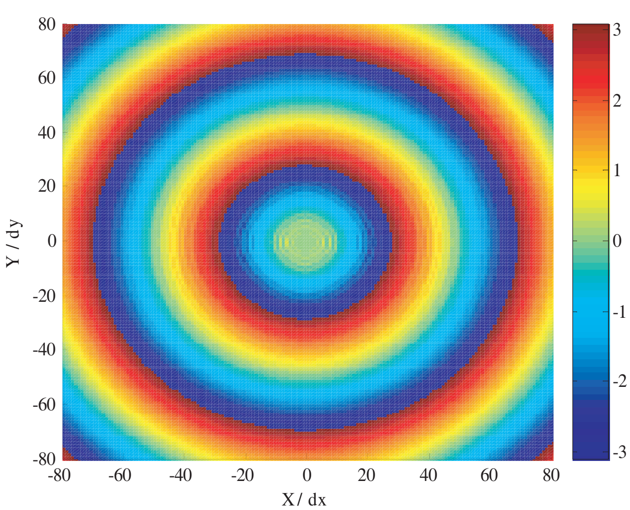

Figure 6. The radiation phase distribution of E_z at $z = 0$ plane with source at $(0, 0, 0)$.

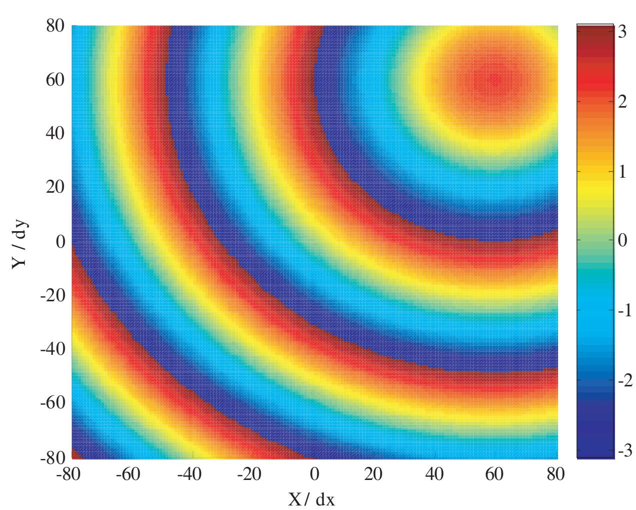

Figure 7. The radiation phase distribution of E_z at $z = 0$ plane with source at $(60, 60, 60)$.

phase distribution of E_z component at the xoy plane when the sinusoidal source is located at the center point $(0, 0, 0)$, and Fig. 7 shows the radiation phase distribution of the E_z component at the xoy plane when the sinusoidal source is located at the center point $(60, 60, 60)$. The CFL number $CFLN$ is set to 4.0. No clear distortion of phase distribution in the computation domain is seen, demonstrating efficient absorbing performance for LOD5-FDTD UPML method.

4. CONCLUSIONS

In this paper, the uniaxial anisotropic perfectly matched layer (UPML) absorbing boundary condition (ABC) in unconditionally stable five-step locally one-dimensional finite-difference time-domain (LOD5-FDTD) method is presented. Relative errors are analyzed at different CFLN conditions. The relative error of the proposed method is compared with the conventional FDTD method and CPML method at CFLN = 1. The result shows good agreement with the conventional FDTD method and nearly -15 dB smaller than the CPML method on average. Comparing Fig. 2 with Fig. 3, it can also be observed that the relative error of the proposed method is still nearly -15 dB smaller than the CPML method on average when CFLN = 4, 9 at the observation point $E_z(0, 10\Delta y, 0)$. The refection error performance of all the three observation points illustrates that the proposed UPML-ABC has good absorption effect. However, the advantage of the LOD-FDTD UPML is its applicability at higher CFLN. To further validate the stability and absorption efficiency of the proposed method, the radiation phase distribution of a sinusoidal source is studied. No clear distortion of phase distribution in the computation domain is seen, demonstrating efficient absorbing performance for the propose UPML method. This development of UPML for the three-dimensional LOD5-FDTD method will enhance applications of the FDTD method.

ACKNOWLEDGMENT

This work is supported by the National Natural Science Foundation of China under Grant (No. 61072002), Elitist of Liu-Da Summit Project in Jiangsu Province at 2011 under Grant (No. 2011-DZXX-031), and graduate research innovation (KYXX_0034). LC acknowledges the support of NSF grant AGS-1405041.

REFERENCES

1. Saxena, A. K. and K. V. Srivastava, "A three-dimensional unconditionally stable five-step LOD-FDTD method," *IEEE Trans. Antenna Propag.*, Vol. 62, No. 3, 1321–1329, Mar. 2014.
2. Courant, R., K. Friedrichs, and H. Lewy, "On the partial difference equations of mathematical physics," *IBMJ*, Vol. 11, 215–234, Mar. 1967.
3. Namiki, T., "A new FDTD algorithm based on alternating-direction implicit method," *IEEE Trans. Microw. Theory. Tech.*, Vol. 47, No. 10, 2003–2007, Oct. 1999.
4. Zheng, F., Z. Chen, and J. Zhang, "A finite-difference time-domain method without the Courant stability conditions," *IEEE Microw. Guided Wave Lett.*, Vol. 9, No. 11, 441–443, Nov. 1999.
5. Tan, E. L., "Unconditionally stable LOD-FDTD method for 3-D Maxwell's equations," *IEEE Microwave and Wireless Components Letters*, Vol. 17, No. 2, 85–87, Feb. 2007.
6. Ahmed, I., E. K. Chua, E. P. Li, and Z. Chen, "Development of the three dimensional unconditionally stable LOD-FDTD method," *IEEE Trans. Antenna Propag.*, Vol. 56, No. 11, 3596–3600, Nov. 2008.
7. Do Nascimento, V. E., B. H. V. Borges, and F. L. Teixeira, "Split-field PML implementations for the unconditionally stable LOD-FDTD method," *IEEE Microwave and Wireless Components Letters*, Vol. 16, No. 7, 398–400, Jul. 2006.
8. Ahmed, I., E. Li, and K. Krohne, "Convolutional perfectly matched layer for an unconditionally stable LOD-FDTD method," *IEEE Microwave and Wireless Components Letters*, Vol. 17, No. 12, 816–819, Dec. 2007.

9. Gedney, S. D., "An Anisotropic perfectly matched layer-absorbing medium for the truncation of FDTD lattices," *IEEE Trans. Antenna Propag.*, Vol. 44, No. 12, 1630–1639, Dec. 1996.
10. Sun, W., N. G. Loeb, and Q. Fu, "Finite-difference time domain solution of light scattering and absorption by particles in an absorbing medium," *Appl. Opt.*, Vol. 41, 5728–5743, Sep. 2002.
11. Sun, W., H. Pan, and G. Videen, "General finite-difference time-domain solution of an arbitrary electromagnetic source interaction with an arbitrary dielectric surface," *Appl. Opt.*, Vol. 48, 6015–6025, Nov. 2009.
12. Wei, B., S. Zhang, F. Wang, and D. Ge, "A novel UPML FDTD absorbing boundary condition for dispersive media," *Waves in Random and Complex Media*, Vol. 20, 511–527, Aug. 2010.
13. Liang, F. and G. Wang, "Study of Mur's and UPML absorbing boundary condition for the LOD-FDTD method," *ICMMT*, Vol. 2, 947–949, 2008.
14. Ahmed, I., E. H. Khoo, and L. Erping, "Development of the CPML for three-dimensional unconditionally stable LOD-FDTD method," *IEEE Trans. Antenna Propag.*, Vol. 58, No. 3, 832–837, Mar. 2010.
15. Omar, R., "Efficient LOD-SC-PML formulations for electromagnetic fields in dispersive media," *IEEE Microwave and Wireless Components Letters*, Vol. 22, No. 6, 297–299, 2012.
16. Taflove, A. and S. C. Hagness, "Computational electrodynamics the finite-difference time-domain method," 3rd Edition, 293, Norwood, MA, Artech House, 2005.